Talanta 89 (2012) 441–447

Contents lists available at SciVerse ScienceDirect

Talanta

journal homepage: www.elsevier.com/locate/talanta

Development and characterization of an electrostatic particle sampling system for the selective collection of trace explosives

Sebastian Beer[a,b,*], Gerhard Müller[a], Jürgen Wöllenstein[b]

[a] EADS Innovation Works Germany, EADS Deutschland GmbH, D-81663 München, Germany
[b] University of Freiburg, IMTEK, D-79085 Freiburg, Germany

ARTICLE INFO

Article history:
Received 11 August 2011
Received in revised form
19 December 2011
Accepted 22 December 2011
Available online 28 December 2011

Keywords:
Trace detection
Particle sampling
Explosives detection
Electrostatic particle precipitator

ABSTRACT

Detection of trace explosives residues at people and cargo control points has become a key security challenge. A severe obstacle is that all commercial and military high explosives have low to extremely low vapor pressures which make them very hard to detect. With detectable vapors not being present, explosives detection needs to proceed through a series of sequential steps including particle collection, thermal vapor conversion and vapor detection. The present paper describes the design and test of an electrostatic particle precipitator which allows particle residue to be collected from the environment, the collected particle residue to be separated into high- and low-electron affinity fractions and the high-electron-affinity one to be concentrated onto a small-area collector surface for later vaporization. The selectivity of this particle collection and separation process is demonstrated and a full-chain demonstration of a DNT detection experiment is presented (DNT: di-nitro-toluene).

1. Introduction

Development of new types of explosives detection systems, particularly for the inspection of cargo and passenger traffic, has become highly significant due to increasing terrorist activity around the world [1–5]. This has caused the European commission to make the enhancement of explosives security a priority issue [6]. The Congressional Research Service of the United States came to a similar conclusion [7]. Currently, dogs are the state of the art in explosives detection, but their attention spans are measured in only tens of minutes [8]. As a consequence, the target for many current research activities is the development of electronic trace explosives detection systems that can match the detection capabilities of dogs while allowing for continuous use for long periods.

While developers have produced trace explosives detectors with high sensitivity and selectivity, the currently available sensor periphery does not match the sensors in fidelity. The performance of detectors may therefore be limited by their sampling systems. According to the head of the U.S. Department of Homeland Security's Transportation Security Lab, S.F. Hallowell, "Chemists have been so fixed on detector development [that] that's exactly what we got: very well-developed detectors that have no front ends. We're going to have to reach out to other disciplines to develop novel sampling systems." [9] In the following work, we report on our progress in the development of a sampling system suitable for field detection of trace explosives residues.

In the case of electronic noses, gas phase detection of explosives has proven to be difficult. Detection of low vapor pressure explosives gases such as TNT, RDX, or PETN, is not applicable since their vapor concentrations are extremely low. However, detection is possible after a certain refashion of sensing and/or preconcentration elements [10]. In this paper we report on our progress in the development of an electrostatic particle sampling system. Trace analyte particles are collected and concentrated on a small substrate, facilitating the transfer into a thermal desorption unit. There the analyte is converted into the gas phase at a temporarily higher concentration which allows for gas detection. We show that ion mobility spectrometry (IMS) is a suitable detection method to be coupled with our sampling system.

2. Background

As stated above, the gas phase detection of explosives is difficult due to their low vapor pressure. In field detection, the already low vapor pressure of explosives has been found to drop even further when improvised explosives devices (IED) are sealed, which is almost always the case. Further problems are innocent compounds which act as interfering species and the lack of mass detection [11]. However, Fair et al. have shown that RDX and TNT detection performance was hugely improved with particle-gas conversion [8]. This indicates that collecting the target substance in particle form,

* Corresponding author at: EADS Innovation Works Germany, EADS Deutschland GmbH, D-81663 München, Germany. Tel.: +49 89 607 21074; fax: +49 89 607 24001.
E-mail address: sebastian.beer@eads.net (S. Beer).

0039-9140/$ – see front matter © 2012 Elsevier B.V. All rights reserved.
doi:10.1016/j.talanta.2011.12.059

with subsequent desorption, may be a more suitable approach for explosives detection.

To date the most effective particle collection method is to accumulate them on a clean surface by wiping, followed by a volatizing step that transports the particles into the detector [8]. A number of different sampling approaches have been developed to improve on this method. For example, Harvey et al. report on a selective preconcentrator for explosives, with direct IMS detection. It features quartz fiber filters with metal β-diketonate polymer impregnation. Saturation is achieved after 24 h of sampling for TNT. RDX is also possible, but takes significantly longer, on the order of months. However, field experiments show that although direct gas phase detection of TNT and RDX gases was not possible, successful detection was performed when using the preconcentration method [12]. A further example is the Sandia Screen Preconcentrator, a system that draws in air or takes a wipe sample, collects the particles in a metal felt, and then resistively heats the felt to desorb the particles. During the heating phase a second air stream which is much lower is used to transport the gas phase analyte to the detector to reduce sample dilution [13].

One potential detection method for explosives gases is IMS. Here, the analyte is identified by determining its electrical mobility, which has been shown to be a characteristic property. The gas is first ionized, usually through the use of a radioactive ionizing source. The ions' electrical mobilities are then determined by measuring their drift time along a drift tube with a defined electrical field [14]. IMS is performed in air at ambient pressure; therefore no vacuum technology is required. This enables IMS technology for field detection [15]. Explosives gases have been shown to lead to strong responses in IMS detectors [16]. Concerning the selectivity of IMS, in the work of Matz et al. IMS was shown to be robust against a set of 17 potential interferent species, although the presence of a contaminant did affect the detector performance by decreasing the sensitivity [2].

At the core of an electrostatic precipitator is a corona discharge. Essentially this creates a unipolar region with ions close to a highly curved electrode with the ions and the electrode both having the same polarity. The charge from these ions can then be transferred to the surface of particles crossing the corona discharge [17]. Corona discharges have been studied thoroughly and detailed explanations of their mechanisms are available [18–20].

The only manifestation of the corona discharge outside the ionization layer is the flow of monopolar ions with the same polarity as the voltage applied to the stressed electrode [21]. For particle precipitation, charge is transferred from an ionized gas to a particle if its electron affinity is higher than the gas electron affinity [22]. One definition of electron affinity is the amount of energy released in the reaction $AB + e \rightarrow AB^- + energy$ at room temperature [23]. This leads to electrostatic precipitators [24,25]. The trajectories of the charged particles are then affected not only by the fluid dynamic force of the transport flow but also by the electrostatic force of the electric field. If the flow and field are matched appropriately, the electric force can dominate and be used to selectively precipitate the charged particles while allowing the uncharged particles to pass. ESPs are used in a many different applications, often as particle filters where the aim is to create a particle-free exhaust flow [26–31].

3. Design

The principal arrangement of the precipitator is shown in Fig. 1. A pump is used to create an airstream that draws the analyte particles through the ESP. Inside, the air entering from the side inlets passes through a corona discharge wire array. A negative high voltage is applied to the corona wires, which along with the opposing collector electrode (at high positive voltage) creates an electric field. As described above this field triggers a negative corona discharge. The negative ions created in this discharge travel from the discharge wires to the collector electrode. When particles travel through this region charge may be transferred from the ions to their surfaces. If the surface charge is sufficient, the hydrodynamic force from the flow is dominated by the electrostatic force. Since the two forces act in opposite directions, the charged particles are moved in opposite direction to the collector surface than the uncharged particles which travel to the exhaust.

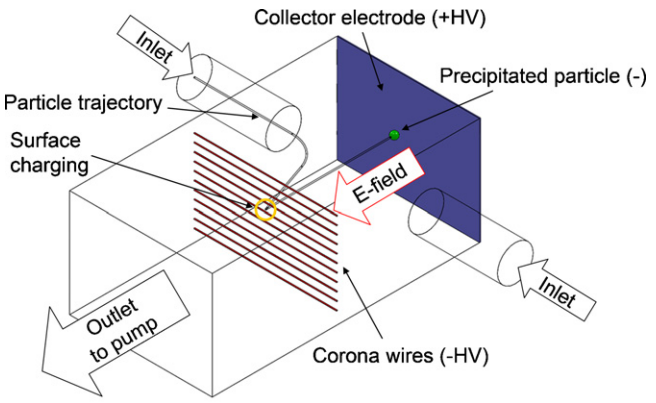

Fig. 1. Schematic of the electrostatic sampler showing an approximated trajectory of a charged particle.

At the collector surface, a passivating layer is placed to prevent the charged particles from releasing their charge, causing them to be electrostatically trapped. In this way particles are accumulated on the collector as more particles are drawn through the ESP. When the collection phase is finished, the potential is no longer applied, and the collector plate is removed to allow for transfer of the particles to a thermodesorber.

As the electrostatic component of the sampler is most critical, the field must be designed carefully. For a corona discharge, the local electric field strength at the highly curved electrodes must be sufficient for breakdown, while the field strength in the remaining corona region must be below the breakdown strength. Air ionization can only occur above a critical field strength; a further increase of the electric field results in a divergent electric field due to the strong repelling force between the ions [21].

For the design of the corona discharge electrodes, the shape of the unipolar region of a single wire electrode was considered [32]. Since a rather large channel size on the order of several cm was chosen to facilitate a large airstream, it was decided that multiple discharge electrodes would be necessary to adequately cover the precipitation volume with ions. However, it is known that a multipoint-to-plane corona differs from a single point arrangement since the adjacent space charges interact [33]. In order to determine the appropriate electrode number and spacing for the array, FEM simulations were performed as shown in Fig. 2. The models indicated that for multiple electrodes (Fig. 2a), a reduction of maximum electric field strength by a factor of about 3 occurs for the wires on the inside of the array. However, adding further wires does not significantly affect this reduction. It is therefore concluded that if an array of more than 2 wires is to be used, the maximum number can be chosen. Secondly, the wire spacing (Fig. 2b) has a significant effect on the maximum field strength. Modeling several wire spacings showed a curve of diminishing effect, with large field reductions at small spacing and little effect at large spacing. For the 300 μm diameter wires to be used in the array, a characteristic length of approximately 4 mm was calculated when the field attenuation was fitted with an exponential function. This characteristic length was chosen as the wire spacing as a compromise between

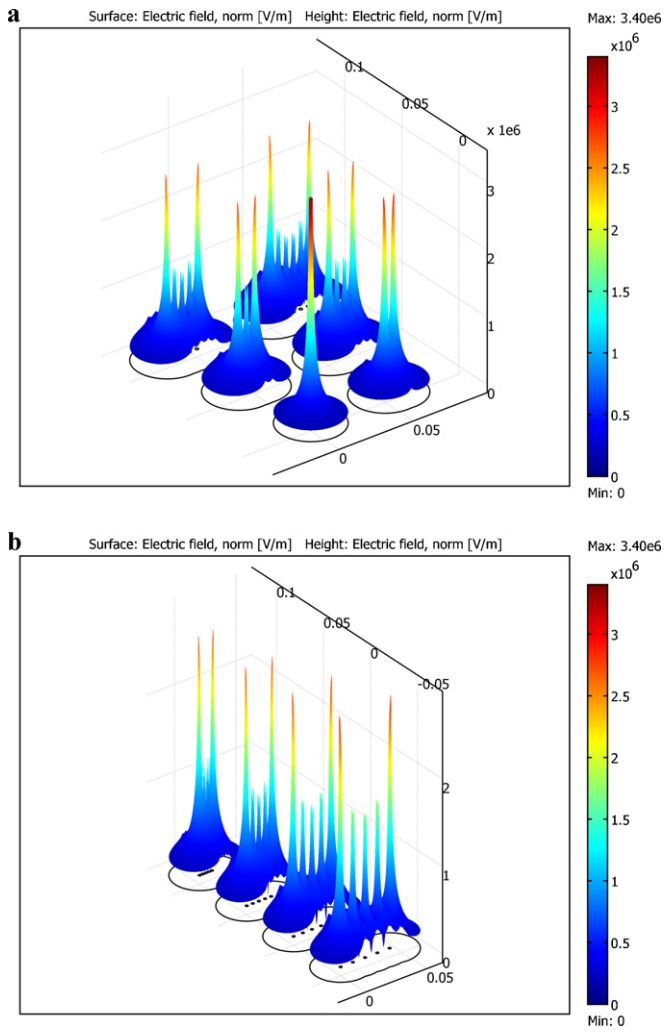

Fig. 2. FEM simulation of the electric field strength for wire arrays with (left, a) increasing wire number and (right, b) increasing spacing when a potential of 10 kV is applied.

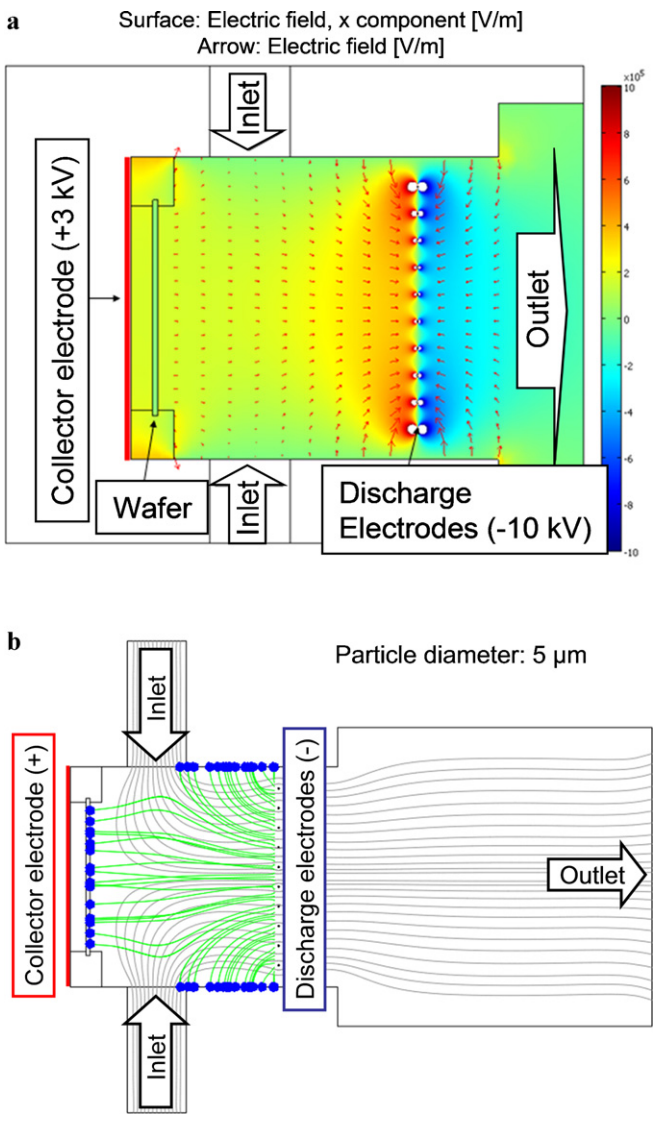

Fig. 3. (Left, a) 2D FEM simulation of the electric field inside the ESP; (right, b) 2D FEM simulation of charged particle trajectories inside the ESP, taking into account an electrostatic force for saturation surface charge as well as a hydrodynamic force from a laminar flow.

field reduction and coverage of the channel. For the 5 cm channel width, this corresponds to a wire array with 10 wires.

For choosing the appropriate electric potential to create the field, it was considered that an increase in the electric field strength also causes an increase in the particle charging [34]. However, the corona mechanism only functions if full breakdown of the air is prevented. The electric field inside the channel was therefore simulated with a range of wire voltages to determine if a sufficient field for a spark channel between the wires and the channel walls or the collector electrode could be present. The breakdown field strength of the air was calculated according to the formulas used by Jullian [35]. It was decided that the walls should be grounded to prevent trapping of charged particles there. Grounded walls allow for discharging of the particles, which then can re-enter the airstream for another precipitation attempt. This requires the collector electrode to be at a positive potential. Fig. 3a shows the FEM simulation of the electric field chosen for the demonstrator, with a high electric field that should not cause full breakdown.

For the electric field considered, charged particle trajectories were simulated to determine if the sampler was designed in a way that allows the electrostatic force to dominate over the fluid dynamic force for charged particles. A saturation charge according to the Weisz limitation of 10^{12} e/cm^2 [36] was assumed. For the air flow, a pressure difference of 0.1 Pa was considered. Fig. 3b shows a sample model for a range of charged particle trajectories. It shows that for a significant range of starting locations the charged particles should be able to reach the collection surface. Some particles travel along trajectories that lead them to the grounded channel walls. However, these particles may release their charges there and then return to the discharge for a further precipitation attempt.

The completed sampler can be seen in Fig. 4. It features aluminum channels and PEEK enclosures for the corona electrodes. A slider holds an oxidized Si wafer plate that serves as a collection surface. For the air stream suction, a handheld vacuum cleaner "Stormy" was attached to the sampler outlet.

4. Experimental results

For the initial performance experiments, TiO_2 particles from Degussa were used. These particles feature a relatively high electron affinity, which should allow for good precipitation in the ESP. This was confirmed in precipitation experiments with varying primary parameters of the sampler. An example for the particle precipitation on the collector plate is shown in Fig. 5:

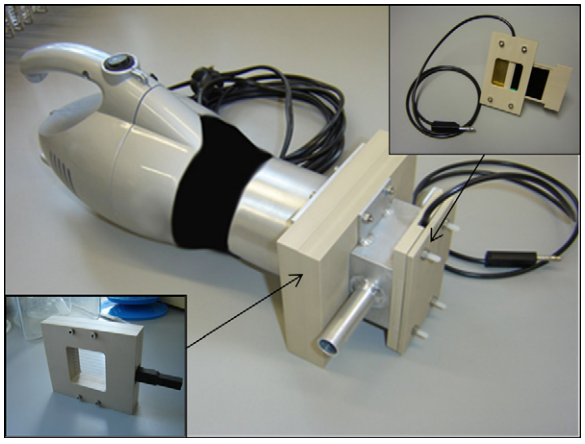

Fig. 4. Sampler assembly, with the discharge wire array (left insert) and the collector electrode and collection substrate wafer (right insert).

4.1. Sampling yield

To determine the effect of the analyte amount on the sampling yield, varying amounts of TiO_2 particles were sampled. The achieved collection yields are shown in Fig. 6. Here it can be seen that the relative yield drops significantly with increasing amount of particles, while the absolute amount collected increases. This indicates that increasing particle coverage on the collector plate reduces the ability of the ESP to further collect particles. Such a saturation effect, in effect, is expected as the negative charge on the collected particles counteracts the applied positive charge on the collector plate.

Since characterizing the amount collected by mass requires a scale, these measurements were difficult to perform for smaller amounts since a sufficiently sensitive scale was not available.

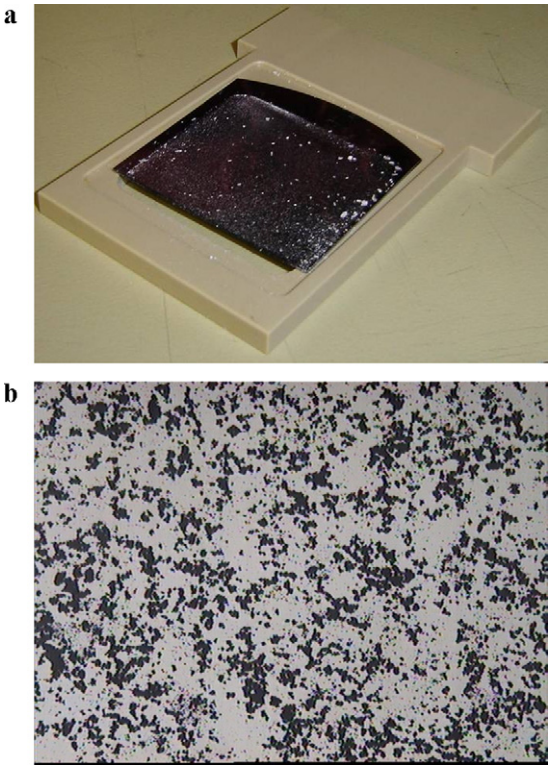

Fig. 5. (Left, a) Precipitated TiO_2 particles on the collector surface, (right, b) microscope image of surface coverage.

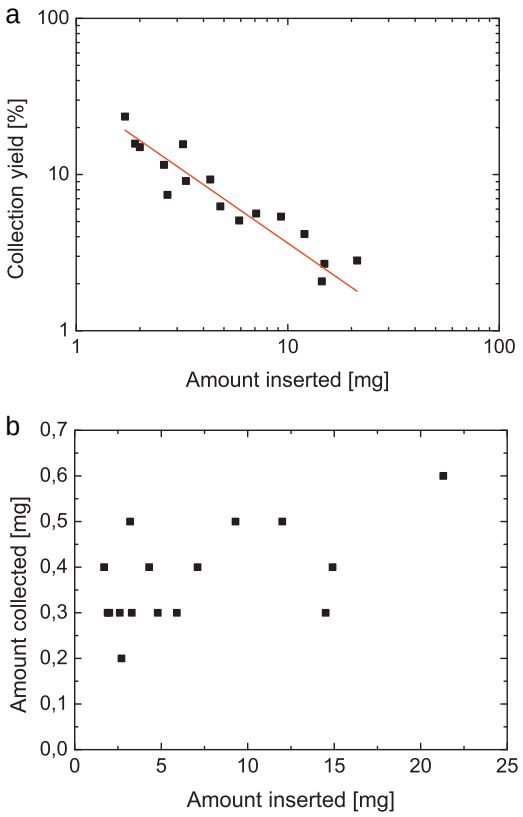

Fig. 6. (Left, a) Collection yield versus inserted amount for TiO_2 particles. Despite an increasing absolute amount, a saturation effect with increasing insertion amount can be seen. The relationship can be fitted reasonably well with a potential function. (Right, b) Amount collected versus amount inserted. It can be seen that the amount collected remains at approximately 0.4 mg regardless of the amount inserted, indicating that the collection has saturated at this amount.

However, an alternative method was used. Microscope images of the collection surface showed the particles in black and the uncovered surface in nearly white. Image processing of the pictures allowed for a full contrast separation of covered and uncovered regions. Converting this black and white image into a grayscale average yields the area coverage. Fig. 7 shows sample black and white images of the collection surface from a reference measurement with no electric field (left) and two collection experiments yielding increasing coverage (center and right). These pictures show that for high yield experiments, a large portion of the surface is covered. Since these particles are still charged, it supports the conclusion that the sampler works better for small amounts. However, it also shows that the amounts that can be sampled are significantly large. They should therefore be sufficient for gas detection after thermal desorption.

4.2. Effect of flow velocity

The effect of the airflow velocity on the sampling yield was determined by varying the pump power with a transformer. This allowed for two inlet air flow velocities of 2.2 and 4.4 m/s, respectively. Comparing the mean wafer coverage for different discharge wire potentials showed that yield is improved by reducing the air flow velocity. However, it should also be noted that currently the suction of the flow is required to draw the particles into the sampler. Obviously reducing the flow also reduces the suction, and a low flow velocity may no longer draw sufficient suction to dislodge and move the particles into the sampler. Fig. 8 shows a comparison of the resulting mean wafer coverage after

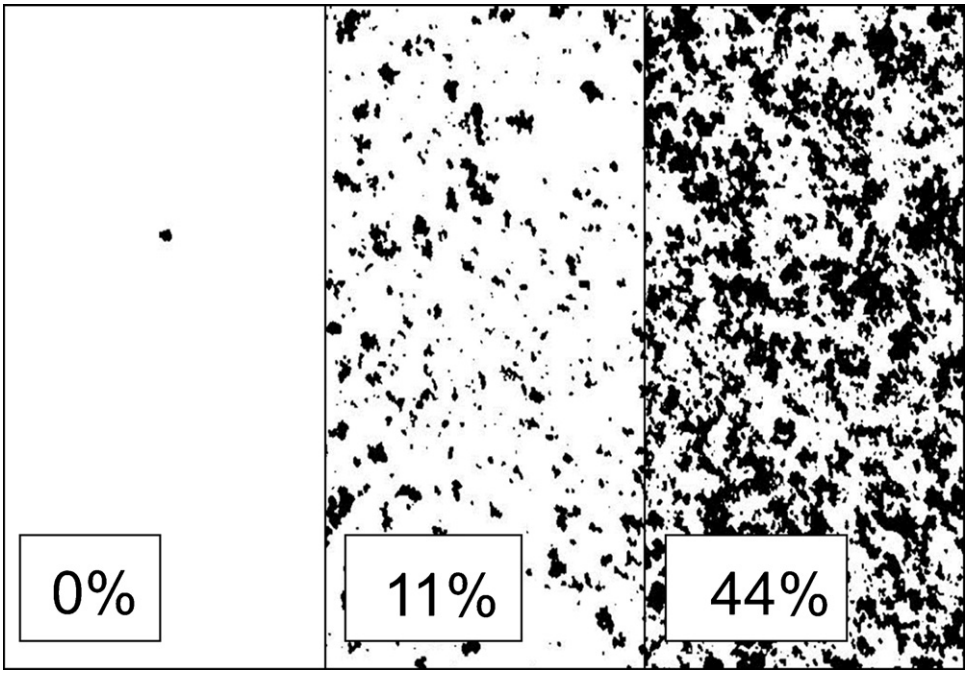

Fig. 7. Images of the collection surface at varying degrees of particle coverage, after contrast conversion to a black and white image. The left portion shows the result from a reference measurement without an electric field, the center and right portions are from measurements with increasing yield.

precipitation for different corona wire voltages and air flow velocities.

4.3. Effect of corona voltage

As stated above, it was to be expected that the collection yield would increase with increasing corona voltage as long as it remained below the sparking potential. This was validated in a set of measurements with varying corona wire voltage at an air flow of 2.2 m/s, as shown in Fig. 9. In the FEM simulations it had been calculated that for moderate ambient humidity, a voltage of −10 kV could be applied to the wires without the occurrence of air breakdown. In the experiments, however, breakdown occurred down to a voltage of −8 kV on the discharge wires. The highest yield with a stable corona was achieved with a wire voltage of −6.8 kV.

4.4. Selectivity experiment

As described in Section 2, the mechanism of charge transfer from the corona-created ions to the particle surface should, in theory, includes a degree of selectivity toward the electron affinity of the particle species. Low electron affinity should not be charged from the ions in the same degree as high electron affinity particles. However, in field conditions there is always a certain amount of humidity present. This presence will result in a water layer forming on the particle surface, changing its surface charging properties. In experiments with wet electrostatic precipitators, where a high degree of humidity is added to the precipitation volume, this effect has been shown to allow for higher particle yields [37]. While this effect is desirable, it raises the question to the degree in which a humidity layer occurring on particles in ambient conditions will affect the potential selectivity of the sampler. Specifically, it must be determined to which extent the yield of low electron affinity species is raised by the humidity alone.

As an estimate to this behavior, an experiment was performed with our ESP where precipitation was performed with a mixture of high electron affinity particles (TiO_2) and low electron affinity particles (ground flour). In theory, primarily the TiO_2 particles should be collected while the flour particles are discarded. As a highly

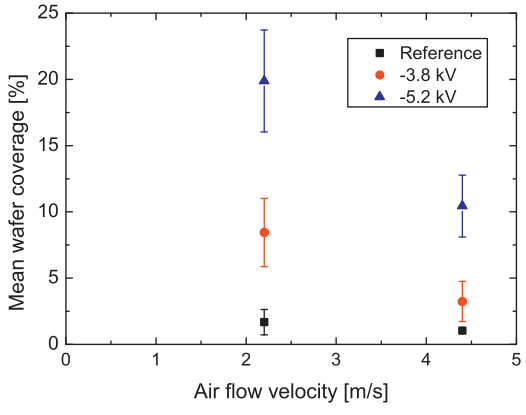

Fig. 8. Comparison of the reference measurements to the measurements with an electric field for a corona wire voltages of −3.8 kV and −5.2 kV.

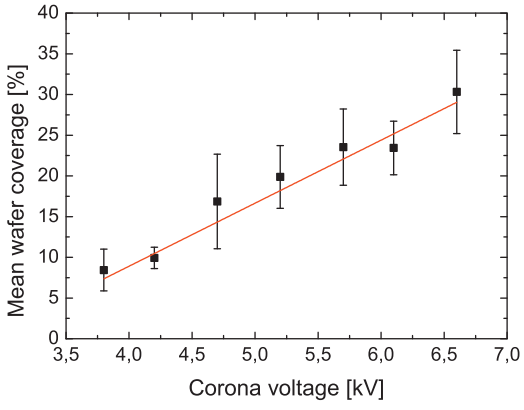

Fig. 9. Mean collector coverage in dependency of the corona wire voltage. Despite the relatively large standard deviations, a linear fit matches the mean data points well.

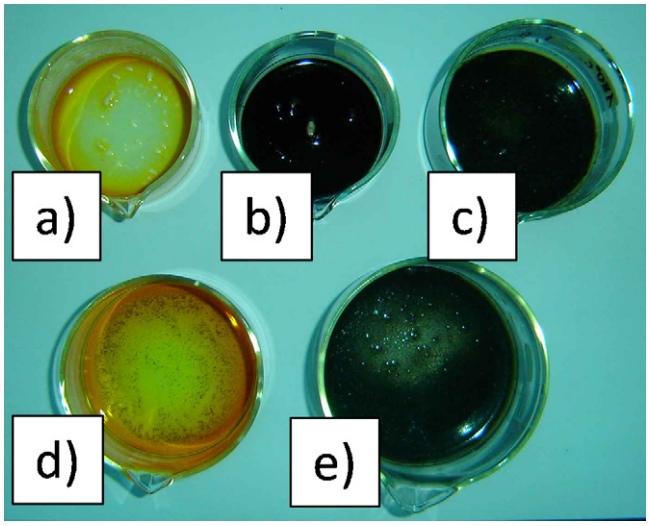

Fig. 10. Lugol's solution samples shown after particle insertion. Top row reference samples: (a) pure TiO_2, (b) pure flour, and (c) TiO_2 and flour mix with flour effect dominating clearly. Bottom row samples from a mixed TiO_2 and flour precipitation experiment: (d) collected particles, (e) discarded particles.

sensitive flour "detector", a Lugol's iodine solution was used. This liquid has the property that it changes from its initial pale transparent yellow color to an opaque dark blue color in the presence of small amounts of starches such as flour [38]. In the top row of Fig. 10, the Lugol's solutions' colors after insertion of TiO_2, flour, and a TiO_2/flour mix can be seen. The liquid turns dark in the presence of flour, regardless of TiO_2 presence.

In the selectivity experiment, a particle mixture of TiO_2 and flour was drawn into the sampler as described in the previous experiments. The particles from the collection surface and the non-collected particles were inserted into separate Lugol's solution samples. As shown in the bottom row of Fig. 10, the collected particle sample remained yellow and clear, indicating that the amount of flour collected was miniscule at most. In contrast, the non-collected particle sample turned dark, confirming the presence of the flour from the mixture. While this result does not certify that no flour was collected, or that no TiO_2 particles were discarded, it does indicate that a degree of selectivity toward the TiO_2 particles was present in the precipitation process. It is assumed that the critical property differentiating the TiO_2 and flour particles is their difference in electron affinity, suggesting that the sampler features selectivity toward high electron affinity particles.

4.5. Full chain demonstration

To demonstrate the validity of the sampling approach, a full chain demonstration was performed using real explosives particles of dinitrotoluene (DNT), the electrostatic sampler, and an Ionscan 500DT IMS from Smiths detection [39]. An amount of 5 mg of DNT particles was placed into a glass dish and subsequently drawn into the ESP with the vacuum suction. Inside the ESP, a small but visible amount (approximately 0.5 mg) was precipitated on the collection plate. Sampled DNT particles can be seen in Fig. 11.

After sampling, the particles were transferred onto a Smiths sampling swab by wiping them off the collection plate with the Ionscan sampling wand. With the wand, the swab is inserted into the Ionscan where the particles are desorbed and analyzed with the Smiths Ionscan IMS. The Ionscan alarmed to 3 explosives species: DNT, NG, and RDX.

The resulting IMS spectrum in the negative (explosives) mode is shown in Fig. 12. Here it can be seen that there is a peak at a drift time of 11.45 ms, corresponding to a mobility value of

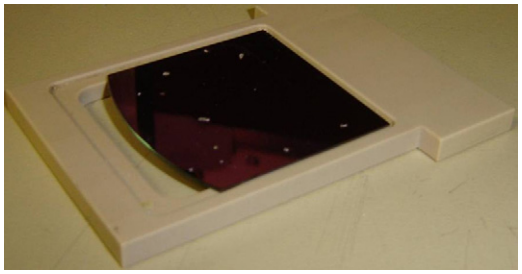

Fig. 11. Precipitated DNT particles on the collection substrate, ready for transfer into the IMS thermodesorber.

$K_0 = 1.5655\ cm^2/(V\,s)$, which is automatically identified by the Ionscan as DNT. Peaks for NG (14.1 ms) and RDX (14.9 ms) were also found. Tracking the peaks over the measurement series shows that the DNT peak arises from the initial desorption. The NG and RDX peaks result from later desorption in subsequent measurements, as seen in Fig. 13.

A reference measurement was performed by directly wiping the DNT particles without a previous ESP step. Again, the IMS identified the substance, confirming the result obtained with the ESP sample.

5. Discussion

Comparing the sampling yield with collection efficiencies of electrostatic aerosol collectors, such as 85–90% for sodium chloride aerosols [40] or 76–94% [31] indicates that there is significant potential for improvement in the yield. However, due to the high sensitivity of the Ionscan detector, the analyte amount collected by our ESP was sufficient for detection.

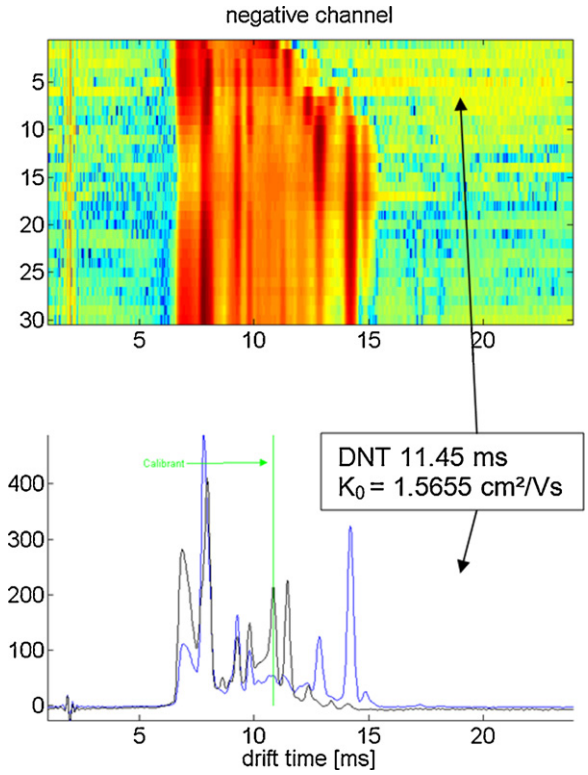

Fig. 12. IMS spectra of ESP-sampled DNT particles, detected with a Smiths Ionscan IMS detector in the negative (explosives-oriented) mode. Shown in black is an initial spectrum, the blue spectrum corresponds to a later measurement. (For interpretation of the references to color in this figure legend, the reader is referred to the web version of the article.)

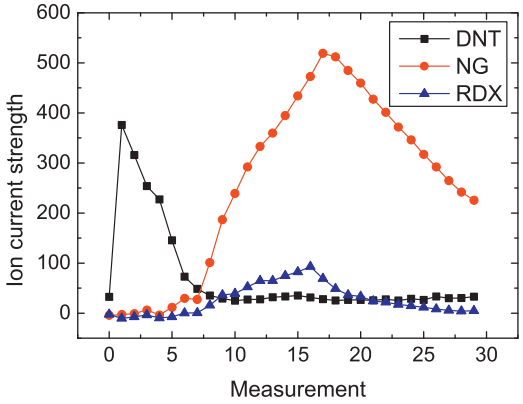

Fig. 13. Signal strength progression for the 3 explosives alarmed by the Ionscan (DNT, NG, RDX). It can be seen that the DNT desorbed relatively quickly while the NG and RDX alarms came from later desorption.

Analysis of the collected particle size distribution showed that the sampler primarily collects relatively small particles. This may be a desirable effect, since smaller particle ranges have been shown to carry a relatively large amount of the information in trace detection. In the work of Fisher et al. [41] in sampling of realistic explosive-containing particle trace, a comparison between the explosives content on smaller and larger particles was made. In the smaller particles composing 25% of the sampled mass, 50% of the TNT amount was found. This indicated that it is better to sample the smaller particles since these contain a relatively larger amount of explosives adsorbed onto their larger surface-to-volume ratio.

6. Summary & outlook

The experiments described above indicate that our approach to sampling and processing trace explosives is suitable for analysis with an IMS detector. Applying electrostatic sampling was shown to introduce a degree of selectivity which improves the detection system performance.

In our future work, we will be improving the sampler performance with a redesign based on our results presented here. The redesign will be realized in a smaller downscaled version to reduce the charged particle trajectory lengths necessary for precipitation and to facilitate stronger electric fields at similar voltages. Furthermore reducing the size of the collection surface will allow for the thermodesorber to be integrated into the collector.

The influence of humidity on the collection efficiency and selectivity will be further investigated. Galbrun et al. showed that the collection efficiency of their ESP was significantly improved with the addition of a small amount of humidity, especially for the smaller particle size ranges [37]. It will be determined how much the particle yield can be improved with a wet ESP, and to which degree the sampler selectivity might be reduced due to the humidity. Furthermore, applicability of the sampler to other types of analyte substances, such as narcotics, will be studied.

References

[1] Y. Tuzkov, in: H. Schubert, A. Kuznetsov (Eds.), Detection and Disposal of Improvised Explosives, 2006, pp. 127–130.
[2] L.M. Matz, P.S. Tornatore, H.H. Hill, Talanta 54 (2001) 171–179.
[3] E.K. Achter, G. Miskolczy, F.W. Fraim, Proc. 1st Int. Symp. Explosive Detection Tech., 1992, pp. 427–434.
[4] S.F. Hallowell, Talanta 54 (2001) 447–458.
[5] R. Lareau, in: H. Schubert, A. Kuznetsov (Eds.), Detection and Disposal of Improvised Explosives, 2006, pp. 289–299.
[6] Council General Secretariat, Implementation of the action plan on enhancing the security of explosives.
[7] 9/11 Commission Report, Final report of the National Commission on Terrorist Attacks upon the United States, W.W. Norton, New York (2004) p. 393.
[8] R.B. Fair, V.K. Pamula, M. Pollack, Proc. SPIE 3079 671 (1997).
[9] A.M. Rouhi, Chem. Eng. News 75 (39) (1997) 24–29.
[10] J.W. Gardner, J. Yinon, Proc. of NATO Advanced Research Workshop on Electronic Noses and Sensors for the Detection of Explosives, Coventry, 2003.
[11] A.V. Kuznetsov, O.I. Osetrov, in: H. Schubert, A. Kuznetsov (Eds.), Detection and Disposal of Improvised Explosives, 2006, pp. 7–25.
[12] S.D. Harvey, E.G. Ewing, M.J. Waltman, Int. J. Ion Mobil. Spec. 12 (2009) 115–121.
[13] D.W. Hannum, K.L. Linker, C.L. Rhykerd, J.E. Parmeter, Proc. 34th IEEE Ann. Int. Conf. Security Technology, 2000, pp. 222–227.
[14] G.A. Eiceman, Z. Karpas, Ion Mobility Spectrometry, 2nd ed., Taylor & Francis, 2005, pp. 121–243.
[15] D.D. Fetterolf, T.D. Clark, Proc. 3rd Symp. Anal. Detect. Explos., Mannheim, 1989, pp. 1–18 (paper 33).
[16] R. Wilson, A. Brittain, in: J.E. Dolan, S.S. Langer (Eds.), Explosives in the Service of Man, Royal Society of Chemistry, Cambridge, 1997, pp. 92–101.
[17] Y.P. Raizer, Gas Discharge Physics, Springer, Berlin, 1991.
[18] L.B. Loeb, Electrical Coronas – Their Basic Mechanisms, University of California Press, Berkeley/Los Angeles, 1965.
[19] B. Held, R. Peyrous, Czech. J. Phys. 49 (3) (1999) 301–320.
[20] M.M. Shahin, in: B.D. Blaustein (Ed.), Chemical Reactions in Electrical Discharges, American Chemical Society, 1969, pp. 48–58.
[21] P. Atten, K. Adamiak, V. Atrazhev, Electrical Insulation and Dielectric Phenomena, 2002 Annual Report on (2002) pp. 109–112.
[22] R. Uttich, Fortschr. Ber. VDI R 3 (381) (1995) 39–55.
[23] A. Zlatkis, C.F. Poole, Electron Capture – Theory and practice in chromatography, Elsevier Scientific, 1981, p. 31.
[24] W.W. Strong, Trans. AIEE 32 (1913).
[25] D. Brocilo, Electrode geometry effects on the collection efficiency of submicron and ultrafine dust particles in wire-plate electrostatic precipitators, PhD Thesis, Open Access Dissertations and Theses, Paper 1290 (2003).
[26] F. Xu, Z. Lou, W. Bo, L. Zhao, X. Gao, M. Fang, K. Cen, J. Electrostat. 67 (2009) 799–806.
[27] C. Ruttanachot, Y. Tirawanichakul, P. Tekasakul, Aerosol Air Qual. Res. 11 (2011) 90–98.
[28] R. Gale, Proc. 11th Int. Conf. Electrostatic Precipitation, 2009, pp. 62–64.
[29] L. Wang, F. Bohe, Proc. 11th Int. Conf. Electrostatic Precipitation, 2009, pp. 19–26.
[30] G. Hermann, G. Lasnitschka, R. Matz, A. Trenin, W. Moritz, Environ. Sci. Pollut. Res. Int. 9 (Suppl. 4) (2002) 83–91.
[31] A. Miller, G. Frey, G. King, C. Sunderman, Aerosol Sci. Technol. 44 (6) (2011) 417–427.
[32] J. Chen, P. Wang, IEEE Trans. Plasma Sci. 33 (2) (2005) 808–812.
[33] A. Jaworek, A. Krupa, Proc. Electromagnetic Devices and Processes in Environment Protection, Lublin, 1997, pp. 209–212.
[34] S.H. Huang, C.C. Chen, Environ. Sci. Technol. 36 (2002) 4625–4632.
[35] M. Jullian, Positive Corona Plasma Electric Field, Boundary Radius and Voltage Drop (Derivation and Table of Values), Blaze Labs Research Group (2004).
[36] C. Canevali, N. Chiodini, P. Di Nola, F. Morazzoni, R. Scotti, C.L. Bianchi, J. Mater. Chem. 7 (6) (1997) 1001.
[37] E. Galbrun, Y. Fouillet, A. Gliere, J. Achard, F. Rouillon, P. Saint-Bonnet, C. Peponnet, Proc. 4th Int. Conf. Tracers and Tracing Methods (Tracer 4), Autrans, France, 2006.
[38] P.C. Sehnke, H.J. Chung, K. Wu, R.J. Ferl, Proc. Natl. Acad. Sci. USA 98 (2) (2001) 765–770.
[39] http://www.smithsdetection.com/IONSCAN_500DT.php (accessed 14.07.11).
[40] Y.S. Cheng, H.C. Yeh, G.M. Kanapilly, Am. Ind. Hyg. Assoc. J. 42 (8) (1981) 605–610.
[41] M. Fisher, C.J. Cumming, M.J. la Grone, R. Taylor, Proc. SPIE 3392 (1998) 565–574.